

Performance Comparison between ImageIR® 8300 hp and ImageIR® 10300 on a Thermoelastic Stress Analysis Experiment

V. Le Saux^{a,*}, S.-A. Wode^b

^aENSTA Bretagne – Institut de Recherche Dupuy de Lôme (IRDLD), FRE CNRS 3744, 2 rue F. Verny 29806 Brest Cedex 9, France

^bInfraTec GmbH – Infrarotsensorik und Messtechnik, Gostritzer Str. 61 – 63, 01217 Dresden, Germany

Abstract

We compare in this document the performance of two infrared cameras (ImageIR® 8300 hp and the ImageIR® 10300), both developed by InfraTec GmbH. The test case is a classical TSA experiment. The results are compared and discussed.

1. Introduction

InfraTec has developed a new infrared camera with better technical characteristics, namely the ImageIR® 10300 camera. However, two properties have risen some questions regarding the thermal resolution, namely the pitch and the dynamic range. The main goal of this report is to give the main results of a short experimental campaign performed at ENSTA Bretagne/IRDLD in Brest (France) by the authors of the document during week 10 aiming at comparing the performance of an ImageIR® 8300 hp available in the IRDL (site of ENIB) and the new ImageIR® 10300 camera. The test case is a Thermoelastic Stress Analysis on the specimen with a hole. This experiment has already been used by one of the authors to compare the performance of various calibration on a product very similar to the ImageIR® 8300 hp, namely the Flir Systems SC 7600BB infrared camera (see [1] for more details). The basic idea is to see if the interrogations are justified or not.

2. Tools and experiments

2.1. Infrared camera

The IRFPA cameras used are InfraTec ImageIR® 8300 hp and ImageIR® 10300. Their main technical characteristic are briefly given in Table 1. The cameras are both equipped with a 50 mm lens (with a HD version for the ImageIR® 10300 camera).

The built-in calibration is used for both cameras and consists of a two-point non uniformity correction coupled to a sophisticated drift compensated DV-to-Temperature conversion algorithm.

2.2. Material, sample and testing conditions

The material used in this section is a standard naval steel. Its Young's modulus E is 210 GPa, the Poisson coefficient is 0.3 and yield stress σ_y is 255 MPa. The sample considered is a plate with a hole: a reminder of its geometrical dimensions is given in Figure 1. More details can be found in [1].

Characteristic	ImageIR® 8300 hp	ImageIR® 10300
Detector	InSb	InSb
Detector format	(640 × 512) IR pixel	(1,920 × 1,536) IR pixel
Spectral range	(2.0 ... 5.0) μm	(3.6 ... 4.9) μm
Pitch	15 μm	10 μm
NETD at 25 °C	25 mK	30 mK
MTTF	8,000 h	10,000 h
Dynamic range	14 bits	13 bits

Table 1: Technical characteristic of the cameras.

Performance Comparison between ImageIR® 8300 hp and ImageIR® 10300 on a Thermoelastic Stress Analysis Experiment

The sample is cyclically loaded with a MTS servohydraulic tension-compression testing machine equipped with a 50 kN load cell. The tests are load controlled at a load ratio $R_\sigma = -1$ at a frequency of 10.02 Hz. The surface of the sample is covered with a high emissivity paint prior to any measurement. The surface temperature of the sample is recorded with the infrared cameras at a frequency of 1 Hz for a duration of about 300 s. This frequency difference with the mechanical loading creates a stroboscopic effect that allows the reconstruction of a mechanical cycle with 50 points.

Figure 2 presents the experimental setup used here. The distance between the cameras and the specimen is chosen such as the entire specimen, plus a small portion of the grips are in the field of view of both cameras. Taking into account the characteristics of both cameras and lenses, the ImageIR® 8300 hp camera is at a distance of 1 m and the ImageIR® 10300 at 50 cm. No specific cautions were taken during the experiment. The idea is here just to compare both cameras (we will see however that the measurements are indeed very good).



Figure 2: Experimental setup. The ImageIR® 8300 hp is on the left, the ImageIR® 10300 on the right and the specimen in between.

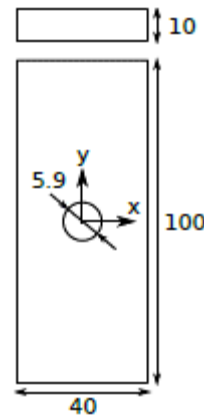


Figure 1: Geometrical characteristic of the sample. All dimensions are given in mm.

2.3. Thermoelasticity

The thermoelasticity theory under cyclic loadings shows that the cyclic temperature amplitude ΔT is proportional to the cyclic change of stresses [2]

$$\Delta T = \frac{\alpha}{\rho c} T_0 \Delta I_1 = k_m T_0 \Delta I_1 \quad (1)$$

where α is the thermal expansion coefficient, ρ the density, c the heat capacity, T_0 a reference temperature, k_m the thermoelastic coefficient, $I_1 = \text{tr}(\sigma)$ is the first invariant of the stress tensor σ and ΔI_1 is the amplitude of the I_1 within the mechanical cycle and is evaluated according to $\Delta I_1 = \max(I_1) - \min(I_1)$.

Even if the sample is cyclically loaded at stress levels lower than the yield stress, the mean temperature of the sample will increase due to the self-heating phenomenon [3]. The temperature variation during the test will therefore be due to the thermoelasticity and self-heating. To be able to apply Lord Kelvin's equation (Equation 1), the self-heating contribution needs to be corrected. We therefore assume that the temperature of each pixel is the sum of three contributions:

Performance Comparison between ImageIR® 8300 hp and ImageIR® 10300 on a Thermoelastic Stress Analysis Experiment

1. An increase in temperature that obeys an asymptotic exponential term (cyclic dissipation is assumed to be constant over the cycles [3]) ;
2. a cyclic temperature change due to thermoelasticity, the form of which is supposed to be the same as the mechanical loading (a sine) ;
3. a constant temperature (i.e. an initial temperature);

The temperature variation evolution, $\theta(t)$, can be modelled, using the following equation

$$\theta(t) = a_c \left[1 - \exp\left(-\frac{t}{b_c}\right) \right] + c_c \sin(2\pi f_{st}t + \varphi) \quad (2)$$

where a_c is the amplitude of the self-heating, b_c is a characteristic time, c_c is the amplitude of the thermoelastic coupling, f_{st} is the stroboscopic frequency, φ is the phase of the sine (assumed to be the same for each pixel). These parameters are identified for each pixel thanks to an optimization procedure. The change in temperature due to the thermoelastic coupling θ_{THE} can then be identified thanks to the relation

$$\theta_{THE}(t) = \theta(t) - a_c \left[1 - \exp\left(-\frac{t}{b_c}\right) \right]. \quad (3)$$

A mean of the minima and maxima is then performed and the difference between these extrema is computed. Based on Equation 1, a ΔI_1 mapping can then be computed and compared to the numerical one. All the processings are performed within a internal custom software developed by V. Le Saux, once the data have been exported from IRBIS® 3.1 software.

3. Results

The results are presented on Figures 3, 4 and 5. Figure 3 presents a mapping of the first stress invariant ΔI_1 for a force amplitude of 20 kN. The numerical results have been mapped using a linear bidimensional method to the ImageIR® 10300 camera in order to ease the comparison of the results. We can notice on the ImageIR® 8300 hp and ImageIR® 10300 mappings some defects (more numerous on the 8300 hp image), related to paint scratches. These scratches obviously do not alter the quality of the measurements outside these areas and have only an impact on the visual look of the mappings.

From a purely visual point of view, we can notice the gain in terms of detector format leads to better resolved gradients. The most interesting point is to see that the reduction of the pitch and of the dynamic range does not lead to a reduction of the thermal sensitivity, which was the main concern evoked in the introduction. We can also notice that the ImageIR® 8300 hp and Flir SC7600 cameras give very similar results, which is fully logical since the sensors are nearly the same (the main difference is related to the digital versus analogical detector design).

In order to provide more quantitative data, x and y profiles are plotted on Figures 4, 5 and 6. These profiles are obtained by plotting the data along the red lines (no mean operation). The experimental results (red symbols) are systematically compared to the FEA results (blue lines). The main conclusion that can be drawn, when comparing the figures, is that the thermal resolution, i.e. the "scattering", is very comparable between the three cameras and that the gradients are better spatially resolved using the ImageIR® 10300 camera (Figure 5).

Performance Comparison between ImageIR® 8300 hp and ImageIR® 10300 on a Thermoelastic Stress Analysis Experiment

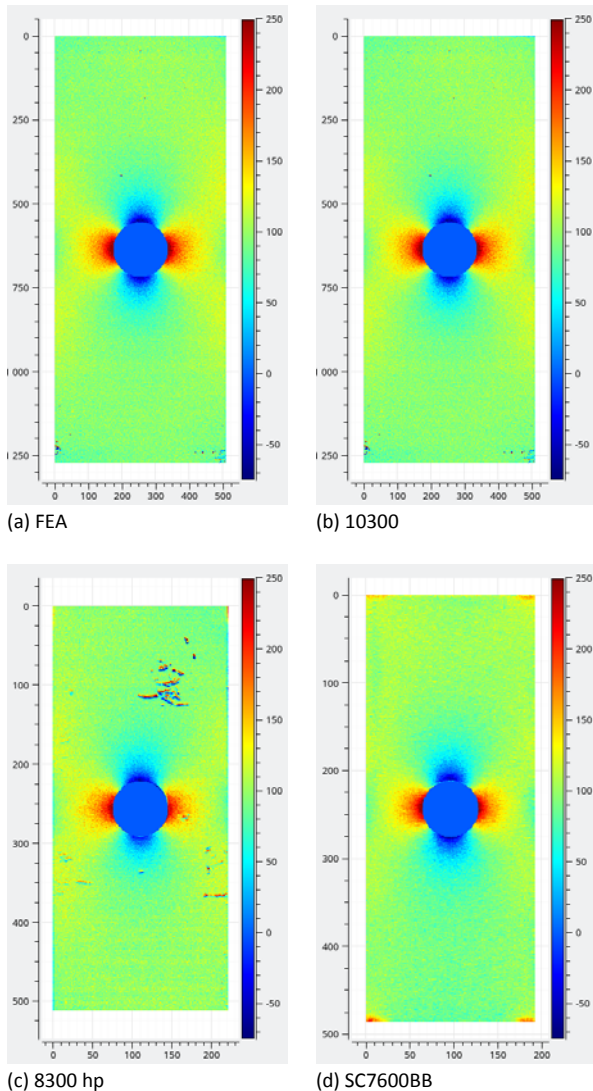


Figure 3: Thermoelastic coupling mapping obtained with (a) the FEA code, (b) the ImageIR® 10300 camera, (c) the ImageIR 8300 camera and (d) the Flir SC7600BB camera.

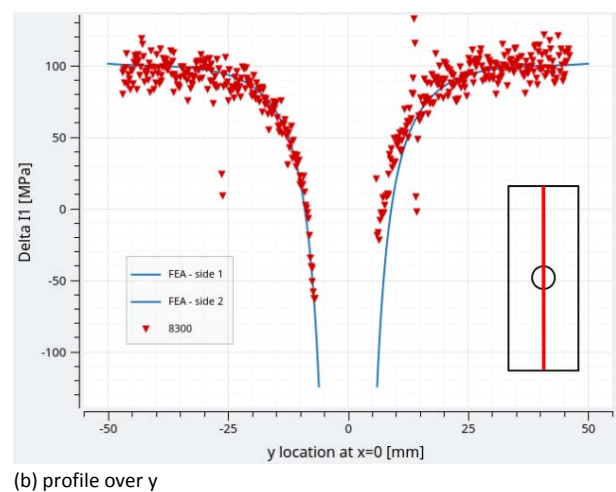
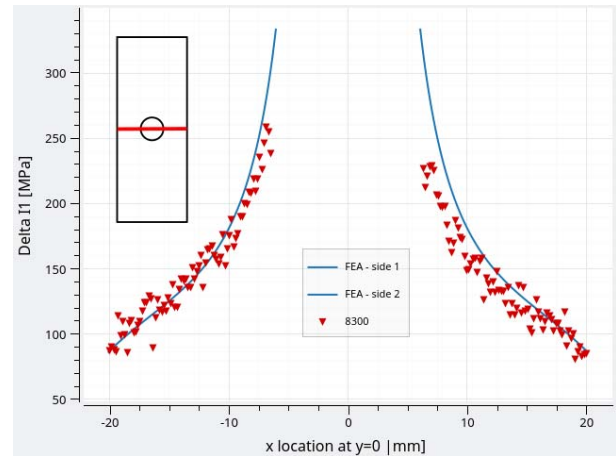


Figure 4: Profiles over x and y for the ImageIR® 8300 hp camera.

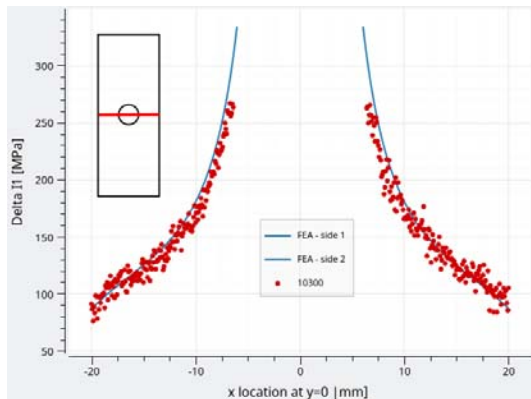
4. Conclusions

In this short communication, we performed Thermoelastic Stress Analysis on three different cameras, including the new ImageIR® 10300. The idea was to challenge this new product and compare its results to the other ones. Based on the results presented, one can conclude that:

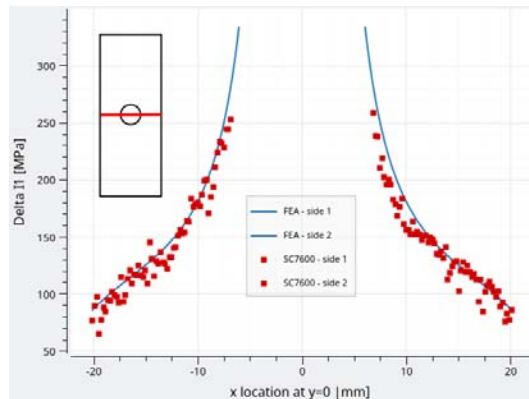
1. Due to the larger detector format and smaller pitch, the gradients are better spatially resolved compared to the results obtained with the ImageIR® 8300 hp and Flir SC7600BB cameras;
2. The thermal sensitivity of the ImageIR® 10300 is very comparable to the other ones, which indicate that the smaller pitch (smaller responsive area) and the lower dynamic digitalization range (13 bits versus 14 bits) does not reduce the quality of the measurements.

Performance Comparison between ImageIR® 8300 hp and ImageIR® 10300 on a Thermoelastic Stress Analysis Experiment

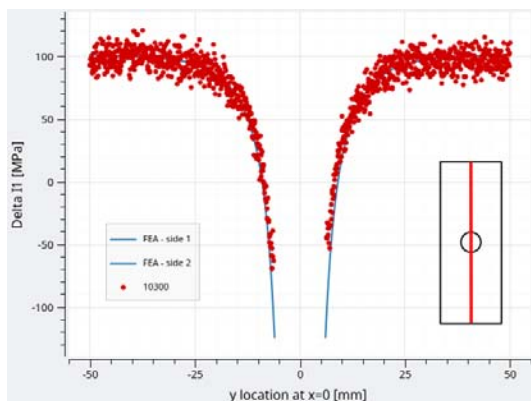
From these results, one can see that the ImageIR® 10300 is a rather impressive product, and that the choices that have been made lead to very promising results.



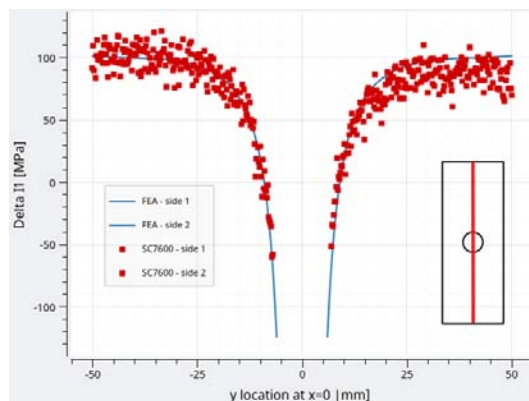
(a) profile over x



(a) profile over x



(b) profile over y



(b) profile over y

Figure 5: Profiles over x and y for the ImageIR® 10300 camera

Figure 6: Profiles over x and y for the Flir SC7600 camera

References

- [1] V. Le Saux, C. Doudard, Proposition of a compensated pixelwise calibration for photonic infrared cameras and comparison to classic calibration procedures: case of thermoelastic stress analysis, *Infrared Physics and Technology* 80 (2017) 83-92.
- [2] P. Stanley, Beginnings and early development of thermoelastic stress analysis, *Strain* 44 (4) (2008) 285-297.
- [3] R. Munier, C. Doudard, S. Calloch, B. Weber, Determination of high cycle fatigue properties of a wide range of steel sheet grades from self-heating measurements, *International Journal of Fatigue* 63 (2014) 46-61.

 *Corresponding author. Tel.: +33 (0)2 98 34 87 18
 URL: vincent.le_saux@ensta-bretagne.fr (V. Le Saux)